Systematic Uncertainties on Δm^2 from Neutrino Physics, using Calorimetric Energy Reconstruction

Deborah A. Harris[a]

[a]Fermi National Accelerator Laboratory
P.O. Box 500 Batavia, Illinois, USA 60510-0500

This report describes how uncertainties in neutrino interactions, particularly at neutrino energies of a few GeV, can contribute to uncertainties in measurements of neutrino oscillation parameters for experiments using calorimetric devices. Uncertainties studied include those on final state multiplicities, cross sections, electron-hadron calorimeter differences, and nuclear rescattering.

1. Introduction

Now that both the solar [1] and atmospheric [2] neutrino anomalies have been confirmed with good confidence with earth-based experiments [3],[4], the next step is to measure precisely the parameters that govern those relatively large effects. The ultimate precision with which the mass splitting between different neutrino types, often denoted as Δm^2, can be determined may limit, among other things, how well the effective mixing angle can be measured. This may even ultimately make the difference as to whether or not CP violation and the neutrino mass hierarchy can be measured. Measuring the mixing angle θ_{23} itself is important also, since how different it is from $\pi/4$ will give us insight into what could be breaking the $\nu_\mu\nu_\tau$ symmetry (consider how different our understanding is because we know now that the long-lived neutral Kaon K_L is not simply an even admixture of K^0 and $\bar{K}^0$!).

In order to determine the neutrino mass hierarchy in the first place, it is important that at least one experiment covers more than several hundred kilometers, and uses neutrino energies above a few GeV. Although water Cerenkov devices have also had a long and glorious history in neutrino physics, calorimeters are likely to be strong contenders for this higher energy regime because they can more completely reconstruct events with many final state particles, which constitue the bulk of the cross section above neutrino energies of one GeV.

In this report we discuss first how calorimeters measure the energies of the final state particles in a neutrino interaction, and then discuss how uncertainties in neutrino interactions, coupled with calorimeter performance, can lead to uncertainties in measurements in oscillation parameters. This report does *not* attempt to evaluate the actual systematic errors arising from these sources, but merely describes how neutrino interaction characteristics will affect the extrapolation from a near to far detector. What this report will also show is that the extent to which these characteristics affect the extrapolation is a function of the mass squared splitting itself.

2. Calorimeters in Neutrino Physics

Calorimetry, loosely defined as segmenting large quantities of passive material with active detectors to measure the passage of charged particles, has played an important role in the history of neutrino physics. Experiments which have used this technique include Frejus [5], CHARM-II [6], Soudan [7], CCFR [8], and /NuTeV [9]. Currently both the MINOS and OPERA detectors are calorimeters (albeit augmented with either a magnetic field or planes of emulsion). By sampling the charged particle flux several times in the course of a hadronic or electromagnetic shower,

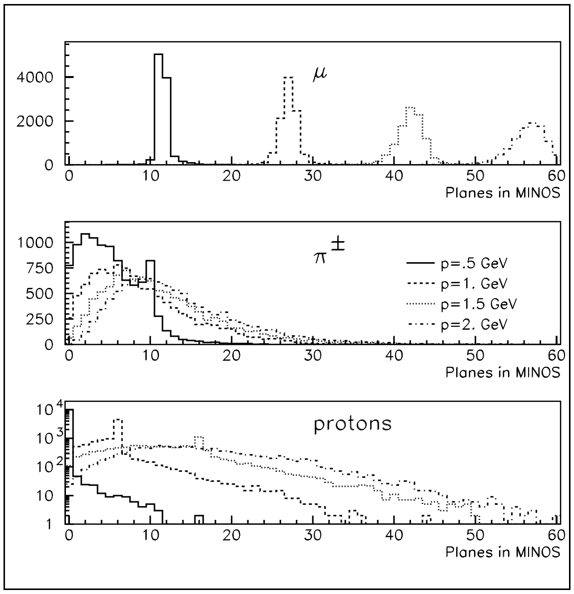

Figure 1. Particle lengths for various particle types and energies, incident on a calorimeter consisting of 2.54cm steel plates separated by 1cm thick planes of scintillator.

one can build a device that gives a very nearly linear response to the "available" (or kinetic) energy of the particle in question. Many aspects of the calorimeter contribute to the response function, including the ratio of responses to electromagnetic to "purely" hadronic interactions. The exact response function versus charged particle kinetic energy is usually measured in a test beam of known momentum and particle composition, since it is difficult to predict precisely. The test beam data can then serve as a check of the validity of the detector simulation, or it can be part of the simulation by providing a library of hadronic and electromagnetic showers.

By making a device with fine segmentation both longitudinally and transverse to an incoming neutrino interaction, a calorimeter can even track multiparticle final states. By using the track lengths combined with the energy depositions of various particles one can determine if they are most likely to be charged pions, electrons, or protons. Figure 1 shows a GEANT prediction for the length distributions for these various particles between 0.5 and 2GeV, for a calorimeter consisting of 2.54 cm steel planes instrumented with 1cm scintillator planes [10]. The muon lengths are on average proportional to the muon kinetic energy, while for pions and protons, a small fraction behave like muons but most have considerably shorter lengths.

3. Neutrino Interaction Simulation

To understand the effects that neutrino interaction uncertainties play in measuring Δm^2 in calorimeters, a simple simulation was used which considered as inputs the NuMI neutrino beam spectra available in the "Low Energy" configuration, shown in figure 2 [11]. Although the event rates may vary, the two kinds of fluxes cover the range of what is being considered: either an on axis neutrino flux which has a very broad range of available energies, or an off axis neutrino flux which is almost monochromatic. The primary motivation for siting a detector off the NuMI beamline axis is to search for $\nu_\mu \to \nu_e$ [12], but given the existence of a detector many times the mass of the MINOS detector at some off axis angle, it will also have a very important role to play in measuring Δm^2 through a ν_μ disappearance measurement. The initial detector which will be located at this off axis location is likely to be a calorimeter, although the longitudinal segmentation (in terms of both interaction and radiation lengths) will be much finer than what is being considered in the analyses described in this report. Furthermore, the nuclear effects may be different, since the detector is likely to be comprised of a lower Z material than the steel assumed here.

For every neutrino event predicted in any near or far detector, the NEUGEN neutrino interaction monte carlo was called [15], with the target assumed to be steel, and final state nuclear interactions turned on ulness noted. The visible energy recorded for each event is simply the kinetic energy of all the final state particles, and the detector is assumed to have perfect energy resolution, to see the neutrino interaction effects before detector smearing. Also, unless noted the detector is assumed to have identical energy response for electromagnetic and hadronic particles, which again is typically not the case. The ratio of electromagnetic to hadronic response varies as a function of energy, but the ratio can deviate from 1 by as much as 30% for many calorimeters [16].

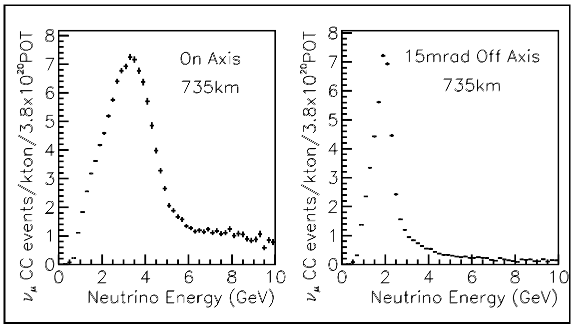

Figure 2. Charged current neutrino event rates for the NuMI Beamline, both on axis (left) and at 15mrad off axis (right), for detectors located a distance of 735km from Fermilab.

4. Signal and Background in Disappearance Measurement

In order to cleanly see an oscillation signature, a calorimeter will have to distinguish between neutral current and ν_μ charged current neutrino interactions. The higher the neutrino energy, the easier this is to do. The most straightforward way to reject neutral current events is to first cut on the length of the longest track in the event, in other words the number of readout planes that were hit for that track. A later step could be to compute a likelihood for that track being consistent with a minimum ionizing particle. Using the distributions shown in figure 1 and NEUGEN the length distributions of neutrino interactions were simulated for the steel-scintillator detector described above. Again this is only a first order estimate of what this distribution might look like, many other detector effects will modify these distributions.

For a given visible energy bin, the length distribution will be very closely related to the y distribution for the ν_μ charged current event sample, where the length is roughly proportional to $(1-y)$. However, the neutral current event length is only logarithmic with the energy of the most energetic pion in the event. Furthermore, at energies below the Δ formation threshold pions are likely to deposit all their energies through dE/dx rather than through nuclear interactions. In those cases, the neutral current length may actually be proportional to the kinetic energy of the leading pion in the neutral current event.

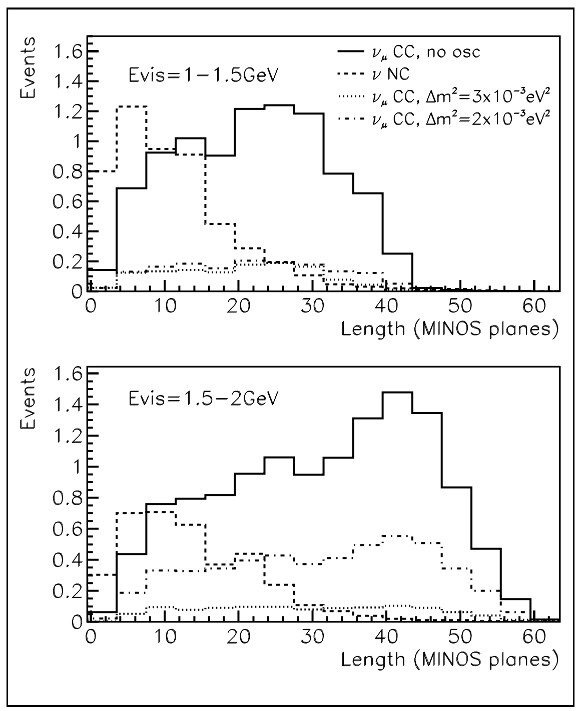

Figure 3. Length distributions for a far MINOS-like detector, for neutral and charged current events, with and without oscillations.

Although monte carlo predictions are that the neutral current background can easily be removed in ν_μ charged current analyses, the precision with which it can be predicted may in fact be limited by how well we understand the y distribution of low energy charged current interactions. This is due to the simple fact that the length distributions in a given energy bin in the near detector will be very different than those in the far detector, in the case of oscillations. Figure 3 shows the lengths in two visible energy bins between 1GeV and 2GeV, for both neutral current and charged current events, with and without oscillations (where the latter would be similar to the near detector length distributions).

Note that for the values of Δm^2 shown, the expected ratio of signal to NC background in the far detector is close to unity at high lengths in these low energy bins, yet in the near detector the high length neutral current events will be swamped even at high lengths by regular charged current events. This neutral current background is dropping rapidly, however, so that at only slightly higher visible energies the neutral current background is much lower. In principle the y distributions could be measured at these higher energies, and then the error on the measurement of the neutral current background would only contain the uncertainty in the extrapolation from moderate (3-4GeV) energy to low (1.5-2.5GeV) energy. However, it should be noted that there is a huge uncertainty in those cross sections themselves, and so large errors may accrue in the extrapolations.

For the remainder of the analyses described in this document, a length cut of 20 (16) planes was placed on events with visible energies greater (less) than 1.5GeV, for both near and far detectors.

5. Multiplicity of Final State Particles

For events with many final state particles, individual particle tracking may be difficult, but the sum of the kinetic energies of the final state particles can nevertheless be measured by the active readout. For high energy neutrinos the difference between the total kinetic energy of the final state particles and the total hadronic energy is negligible, but in the one to two GeV regime, the multiplicity and rest masses of the final state particles become important [13]. The resulting neutrino energy smearing for various energy regions relevant to the NuMI neutrino beams can be seen in figure 4, which shows the distribution of the ratio between the total kinetic and true neutrino energy. This smearing can be reduced for a very fine-grained detector which has good particle ID by including the final state particle rest masses into the energy calculation, as was done with the Soudan detector [14].

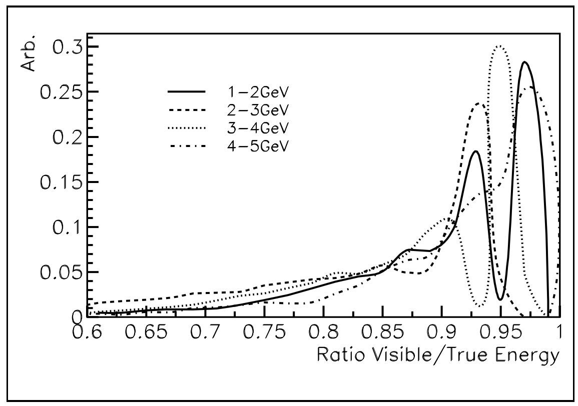

Figure 4. Ratio of visible to true neutrino energy for various energy ranges. The structure in the distribution is due to different multiplicity final states.

To see what the size of the overall effect of "neutrino energy smearing" is, one can compare the predicted ratio of far detector energy spectra with and without oscillations, before and after this neutrino energy smearing. Figure 5 shows this ratio for two different values of Δm^2, for the on axis NuMI beam. Note that the effect will change not only where the dip in the energy spectrum is, but will also change dramatically the height of the dip itself.

If the total reconstructed kinetic energy of the event is a fraction f of the total true neutrino en-

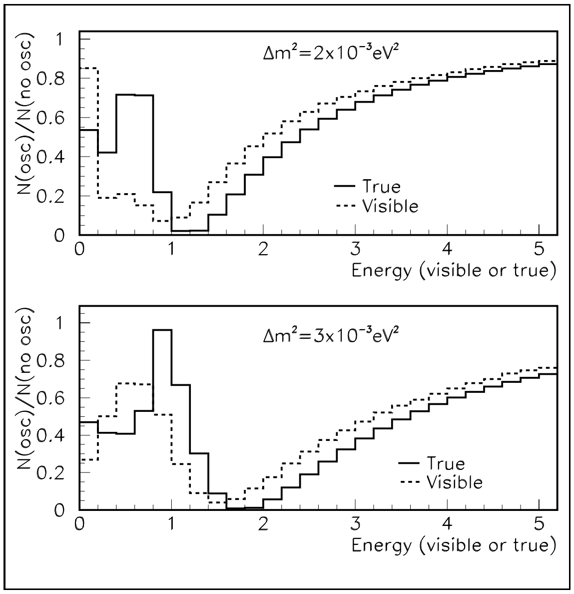

Figure 5. Ratio of far detector event predictions: for the case of oscillations divided by the case of no oscillations. Solid lines indicate the ratio versus true neutrino energies, and the dashed lines indicate the same ratio but as a function of reconstructed neutrino energy.

ergy, then one can study uncertainties in the distribution of f (shown in figure 4) in a simplistic way by changing f to $f + 0.2(1 - f)$, but assuming in the extrapolation from near to far that the near to far ratio does not change. Neutral current and charged current events are treated identically, although a cut on the maximum track length is made to remove the neutral current backgrounds. This is not an appropriate way to evaluate the total systematic error coming from uncertainties in f, but merely an exercise to determine roughly how well one must understand the f distribution. Figure 6 shows how different the predicted far detector energy spectra would be for two values of Δm^2, for the on axis beam, if the smearing were changed in this way. Ultimately this corresponds to about a 3% systematic error in the measured Δm^2, which is less than the expected MINOS error, but well above the next generation proposals. Off-axis neutrino experiments are also subject to this problem, as shown in figure 7 and again a 20% change in the ratio f leads to about a 3% change in the reconstructed Δm^2.

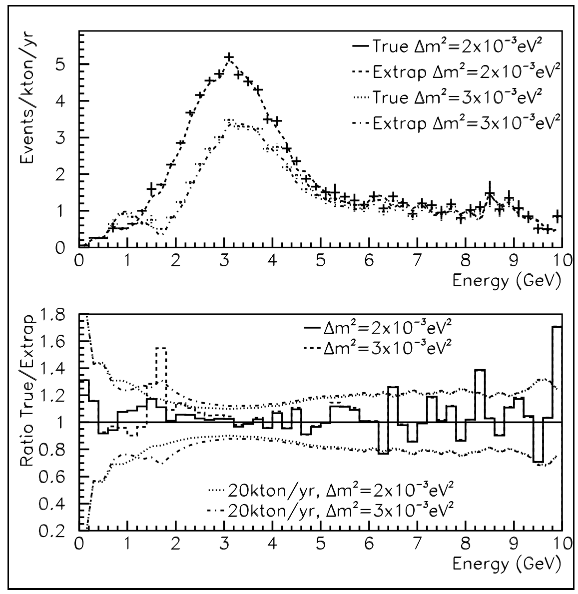

Figure 6. Difference between “true” and “extrapolated” on axis far detector spectra, for the case where the neutrino energy smearing, described in text, is 20% larger than the simulation assumes. Also shown in the lower plot is the ratio of true to extrapolated, for two different values of Δm^2, along with the statistical error on that ratio for 20kton-years of nominal NuMI running.

6. Cross Section Uncertainties

One often hears in discussions of oscillation experiments that the near detector is used to cancel out the cross section uncertainties, since the cross section as a function of neutrino energy should be identical if the two detectors are comprised of the same material. In fact this statement is true

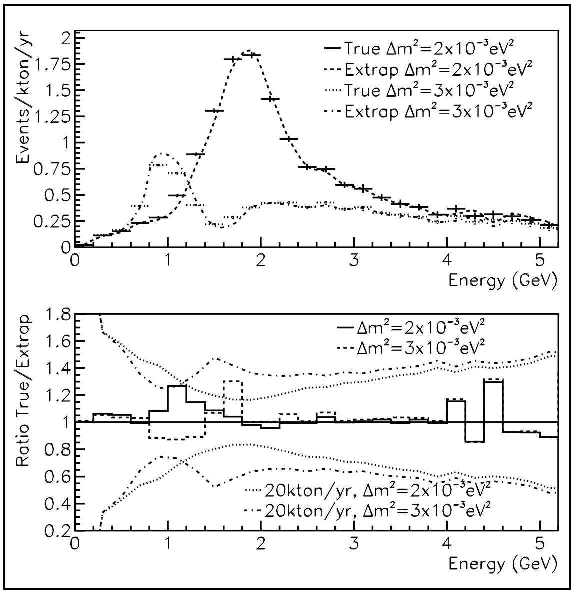

Figure 7. Difference between "true" and "extrapolated" off axis far detector spectra, for the case where the neutrino energy smearing, described in text, is 20% larger than the simulation assumes. Also shown in the lower plot is the ratio of true to extrapolated, for two different values of Δm^2, along with the statistical error on that ratio for 100kton-years of nominal NuMI running.

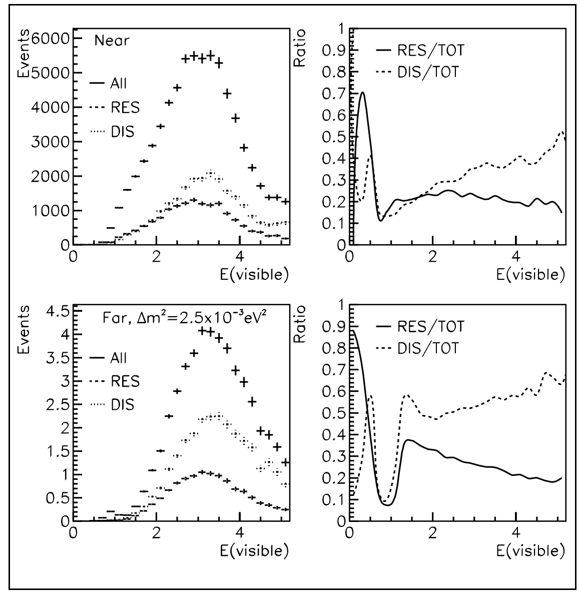

Figure 8. Left: Visible CC energy distribution broken down into the three different components: Quasielastic, Resonance, and Deep Inelastic Scattering; Right: the ratio of Resonance and DIS to the total event rate, at the near detector (top) and far (bottom), assuming oscillations.

only in the limit of a detector in which the visible energy in the detector is identical to the incoming neutrino energy. However, cross sections may change dramatically as a function of energy, and as we have seen, even a perfect calorimeter cannot perfectly reconstruct the actual neutrino energy. Finally, the energy smearing combined with potentially a very large difference between the near and far detector fluxes means that cross section uncertainties can be quite important.

Figure 8 shows visible energy distribution for charged current events after an event length cut is applied to remove neutral current events, and what the relative contributions are of Quasielastic, Resonance, or Deep Inelastic Scattering processes. The top is for the near detector, and the bottom is for the far detector, in the case of oscillations at $\Delta m^2 = 2.5 \times 10^{-3} eV^2$. Note that as expected, the Deep Inelastic Scattering process contributes significantly more to the far detector event rate than that of the near detector, since the lowest energy neutrinos are osclilating to ν_τ events where the charged current interaction does not occur due to the τ mass suppression.

Figure 9 shows the ratios between the "extrapolated" and the "true" neutrino event spectra for the case where the DIS cross section is actually different from what the Monte Carlo assumes by 30%, (left plots), and where the resonance cross section is different by 50% (right plots), and for the on (top) and off (bottom) axis beams shown in figure 2. These are certainly not the uncertainties at high neutrino energies, but for neutrino energies of a few GeV they are not unreasonable. For

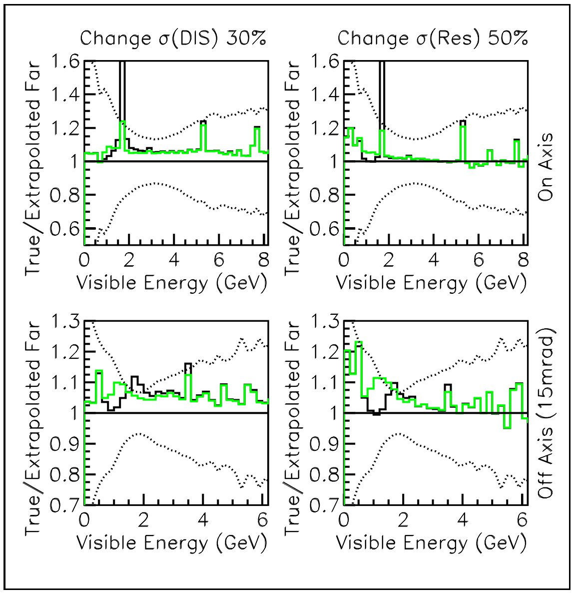

Figure 9. Ratio of true to extrapolated neutrino event rates as a function of visible energy for on axis (top) and off axis (bottom) for uncertainties in DIS (left) and Resonance (right) cross sections. The dark (grey) lines are for $\Delta m^2 = 3(2) \times 10^{-3} eV^2$, and the On (Off) axis statistical errors are shown for 10 (100) kton years.

different values of Δm^2 the far detector prediction can change by up to 5 or 10 per cent, most notably in the locations where the near and far detector event distribution shapes are the most different. Also shown on the plot in dotted lines is the statistical error in each neutrino energy bin assuming 10kton-years for the on axis case, and 100kton-years for the off-axis case. In both cases a length cut is made to reduce the neutral current background, and the detector assumed is a steel scintillator detector. Note that for the off axis case, because of the higher detector mass assumed and the sharper neutrino spectrum, the cross section effects tend to be larger, and in some cases as large as the statistical error in relatively important energy bins. Although in the on axis case the effects are never as large in any single bin as the statistical error, and as such they would not affect the sensitivity on Δm^2, they would contribute to a significantly higher minimum χ^2 on any oscillation fit. Also, note that the systematic errors in these cases are 100% correlated bin to bin, yet the statistical error is completely uncorrelated. So averaging over many (say 10 or 15) high energy neutrino bins would in fact lead to systematic error comparable to the statistical one.

7. Electron-Hadron Differences in Calorimeters

Another effect which has not been studied in detail but which should be mentioned in passing is the fact that calorimeters typically do not on average register the same amount of signal for an electromagnetic and a hadronic particle of the same energy. This is due to the fact that hadronic showers, which can lose energy by electromagnetic processes, also tend to lose energy through transfer to neutrons, which do not leave much signal in a calorimeter. So on average an electromagnetic particle of a certain kinetic energy will leave as much as 30% more signal in a calorimeter than a hadron of the same kinetic energy. When neutrinos are energetic enough to produce either charged or neutral particles in the same final state (i.e. $\nu n \rightarrow \mu^- n \pi^+$ as opposed to $\nu n \rightarrow \mu^- p \pi^0$), the energy measured can vary by up to 30% of the total non-muon energy. These differences could also arise in the predictions of the neutral current backgrounds as a function of visible energy. As an overestimate of the effect, we consider here the difference in the extrapolated far energy spectrum for two scenarios– one where the detector has equivalent electron to hadronic response, and the other where the detector has an electron to hadron response of 1.3. The double ratio of far over near neutrino energy spectra, $(e/\pi = 1.3/e/\pi = 1.0)$ as a function of Δm^2 is shown in figure 10. This seems to be a bigger effect for an on axis beam than an off axis beam. In an on axis beam it has an effect at about one GeV where the spectrum is quickly falling, and for the off axis beam the effect seems to be one mostly of changing the level, not the shape of the near/far extrapolation.

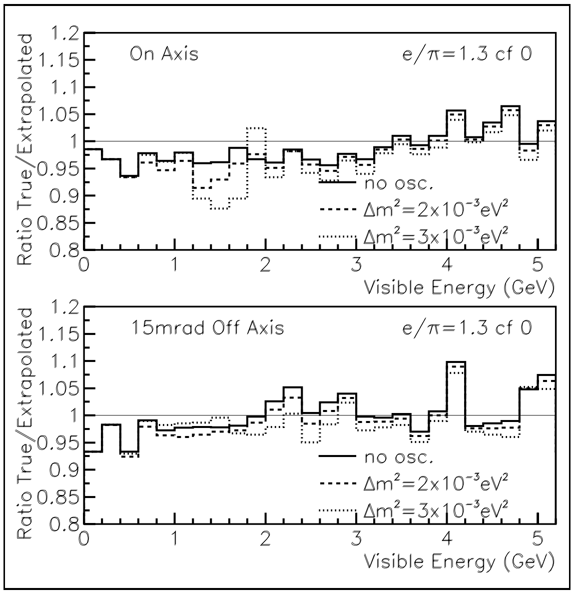

Figure 10. Ratio of true to extrapolated neutrino event rates as a function of visible energy for on axis (top) and off axis (bottom) if one assumes an e/π of 1.3 compared to 1.0.

8. Nuclear Effects

Still another important effect which is related to the visible energy smearing for a given true neutrino energy is nuclear effects. As has been measured in neutrino scattering, there is some probability that a pion produced in a W or Z exchange in a nucleus may be absorbed before it gets out of the nucleus [17]. Of course if that pion is absorbed it will not deposit energy in the calorimeter, resulting in still lower reconstructed energy for a given true neutrino energy. The effect of pions rescattering was included in figures 4 and 5 but if it were not accounted for, the difference in the far over near prediction is shown in figure 11. .

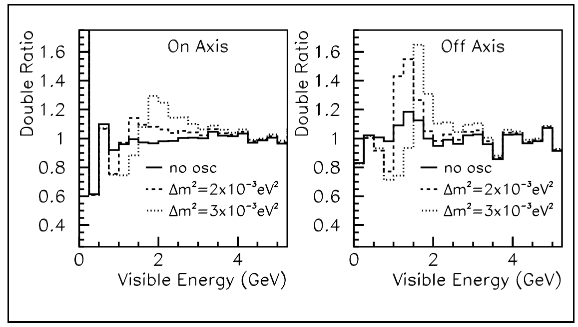

Figure 11. Ratio of true to extrapolated neutrino event rates as a function of visible energy for on axis (left) and off axis (right) if one assumes nuclear rescattering compared to no nuclear rescattering, as modeled in NEUGEN.

9. Conclusions

All of the neutrino interaction uncertainties that will ultimately plague precision measurements of Δm^2 have not been mentioned in this report, however several possible sources of uncertaintes in a calorimetric measurement have been described. Table 1 gives a brief summary of these studies, where for each effect considered the possibility of a shape or a level change in the far detector event rate is noted, for the case of Δm^2 being equal to $2 \times 10^{-3} eV^2$. The most important thing that should be noted is that for most of the neutrino interaction uncertainties considered, the systematic error associated with the far detector prediction depends on what Δm^2 is being assumed. In particular, if one compares the systematic error in the absence of oscillations to that in the presence of oscillations, the errors are always larger in the presence of oscillations, at least when the disappearance probability is large, as is the case for all future proposed experiments. The effects considered can bring about errors in a far detector extrapolation of anywhere from a few per cent to 20 or 30 per cent in a narrow energy window (which tends to be around the 1 or 2 GeV region). It is clear that ultimately to get to precisions of a few per cent on Δm^2 itself, we as a field have to acquire a much better understanding of neutrino interactions and their cross sections.

REFERENCES

1. Q.R. Ahmad *et al*, Phys.Rev.Lett. **89** 011301, 2002 and S. Fukuda *et al*, Phys.Rev.Lett.**86** 5656, 001
2. See for example Y. Fukuda *et al*, Phys.Rev.Lett. **81** 1562, 1998
3. K. Eguchi *et al*, Phys.Rev.Lett.**90** 021802,2003
4. M.H.Ahn *et al*, Phys.Rev.Lett.**90** 041801, 2003.
5. C.Berger *et al*, Nucl. Instrum. Meth. **A262** 463, 1987.
6. D. Geiregat *et al.*, Nucl. Instrum. Meth. **A325** 92 , 1993.
7. W.W.M. Allison *et al.*, Nucl. Instrum. Meth. **A381** 385 , 1996.
8. W.K. Sakumoto *et al.*, Nucl.Instrum.Meth.**A294** 179, 1990
9. D.A.Harris, J.Yu, *et al.*, Nucl. Instrum. Meth. **A447** 377 ,2000.
10. Adam Para, private communication
11. NuMI Beamline Fluxes from Version 14 of GEANT-based MC, courtesy of Mark Messier
12. D. Ayres *et al.*, hep-ex/0210005 October 2002
13. A. Para, proceedings for NuINT01, Nucl.Phys.Proc.Suppl. **112** 9, 2002
14. Hugh Hallagher, private communication
15. G. Barr, D. Phil thesis, University of Oxford (1987), and also H. Gallagher, proceedings for NuINT01, Nucl.Phys.Proc.Suppl. **112** 188, 2002
16. R. Wigmans, Nucl.Instrum.Meth.**A259** 389, 1987
17. R. Merenyi *et al.*, Phys.Rev. **D45** 743,1992

Table 1: The far to near extrapolation change due to various neutrino interaction effects

		On Axis		Off Axis	
	Size of	Type of Change		Type of Change	
Effect Considered	Change	Shape (%)	Level (%)	Shape (%)	Level (%)
ν Energy Smearing	Extra 20%	20% at 1.5GeV	-	25% at 1.0GeV	-
DIS Cross Section	30% off	25% at 2GeV	5%	10% at 2GeV	5%
Resonance Cross Section	50% off	20% at .5GeV	-	10% at 1GeV	-
electron/hadron difference	$1.3 \to 1.0$	10% at 1.5 GeV	3% below 3GeV	-	3% below 2GeV
Nuclear Rescattering	On/Off	25% at 1GeV	-	50% at 1.5GeV	